AD-A035 221 GEORGIA INST OF TECH ATLANTA ENGINEERING EXPERIMENT --ETC F/G 17/9
ENVIRONMENT AND RADAR OPERATION SIMULATOR.(U)
JUN 76 S N COLE, E R FLYNT

UNCLASSIFIED

DAAB07-74-C-0272

ECOM-74-0272-7

NL

1 OF 1
AD A035221

END

DATE FILMED
3-77

RESEARCH AND DEVELOPMENT TECHNICAL REPORT

REPORT ECOM-74-0272-7

ENVIRONMENT AND RADAR OPERATION SIMULATOR

By

S.N. Cole
E.R. Flynt

Engineering Experiment Station
Georgia Institute of Technology
Atlanta, Georgia 30332

June 1976

Seventh Quarterly Report for Period 1 January 1976 through 31 March 1976

Prepared for

ECOM

US ARMY ELECTRONICS COMMAND FORT MONMOUTH, NEW JERSEY 07703

NOTICES

Disclaimers

The findings in this report are not to be construed as an official Department of the Army position, unless so designated by other authorized documents.

The citation of trade names and names of manufacturers in this report is not to be construed as official Government indorsement or approval of commercial products or services referenced herein.

Disposition

Destroy this report when it is no longer needed. Do not return it to the originator.

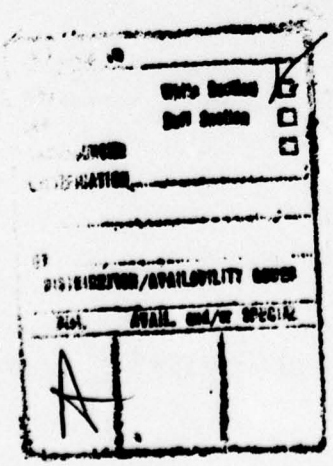

UNCLASSIFIED

SECURITY CLASSIFICATION OF THIS PAGE (When Data Entered)

REPORT DOCUMENTATION PAGE	READ INSTRUCTIONS BEFORE COMPLETING FORM
1. REPORT NUMBER: ECOM-74-0272-7	2. GOVT ACCESSION NO. / 3. RECIPIENT'S CATALOG NUMBER
4. TITLE (and Subtitle): ENVIRONMENT AND RADAR OPERATION SIMULATOR,	5. TYPE OF REPORT & PERIOD COVERED: Seventh Quarterly, 1 Jan 76 - 31 Mar 76
	6. PERFORMING ORG. REPORT NUMBER
7. AUTHOR(s): S. N. Cole, E. R. Flynt	8. CONTRACT OR GRANT NUMBER(s): DAAB07-74-C-0272
9. PERFORMING ORGANIZATION NAME AND ADDRESS: Georgia Institute of Technology, Atlanta, Georgia 30332	10. PROGRAM ELEMENT, PROJECT, TASK AREA & WORK UNIT NUMBERS: DA Proj C8-3-05107-05-C8-CA; AMC Proj 1S7-62703-D-H93-P1-06; AMC Code 672703-12-H93-P1-06
11. CONTROLLING OFFICE NAME AND ADDRESS: Commander, US Army Electronics Command, AMSEL-CT-R, Fort Monmouth, NJ 07703	12. REPORT DATE: June 1976
	13. NUMBER OF PAGES: 14
14. MONITORING AGENCY NAME & ADDRESS (if different from Controlling Office): Quarterly rept. no. 7, 1 Jan - 31 Mar 76	15. SECURITY CLASS. (of this report): UNCLASSIFIED
	15a. DECLASSIFICATION/DOWNGRADING SCHEDULE

16. DISTRIBUTION STATEMENT (of this Report)

Approved for public release; distribution unlimited

19p.

17. DISTRIBUTION STATEMENT (of the abstract entered in Block 20, if different from Report): 1S762703D H93 P1

18. SUPPLEMENTARY NOTES

19. KEY WORDS (Continue on reverse side if necessary and identify by block number)

Signal Synthesis
Clutter Synthesis
Pseudo-Random Numbers
Radar Simulation
Radar Target Simulation
Radar Clutter Simulation
Radar Cross Section Scaling

20. ABSTRACT (Continue on reverse side if necessary and identify by block number)

This report summarizes activities during the seventh quarter of a program sponsored by the U.S. Army Electronics Command (ECOM), directed toward the design of an Environment and Radar Operation Simulator (EROS). In addition some of the analysis results and design decisions are described in detail.

A computer simulation of the shift-register random-number generator has been performed to verify its autocorrelation properties. The implementation decision with regard to radar cross section scaling is presented as a formula, →

(CONTD.)

DD FORM 1 JAN 73 1473 EDITION OF 1 NOV 55 IS OBSOLETE

UNCLASSIFIED 153850

SECURITY CLASSIFICATION OF THIS PAGE (When Data Entered)

LB

ABSTRACT (Contd.)

and the techniques for applying this formula to target and clutter signals are discussed. In previously reported design plans the range weighting and integration functions were to be performed by digital hardware. It has been determined that there are a number of advantages to performing these functions in analog hardware, and the design plan has been modified accordingly.

PREFACE

This report was prepared at the Georgia Tech Engineering Experiment Station under Contract No. DAAB07-74-C-0272. The work covered by this report was performed in the Applied Engineering Laboratory under the supervision of Dr. H. A. Ecker and Mr. J. L. Eaves, Director of the Applied Engineering Laboratory and Chief of the Radar Technology division, respectively. The progress reported herein was performed during the seventh quarter of a program to develop an environment and radar operation simulator (EROS) to be used in testing radar receivers and components.

This project is being monitored by Mr. Reinhard G. Olesch and Mr. Otto E. Rittenbach of the U.S. Army Electronics Command, and their helpful suggestions are acknowledged.

TABLE OF CONTENTS

1. INTRODUCTION

This report covers work performed during the period 1 January 1976 through 31 March 1976, the seventh quarter of a 30-month program to design and build an Environment and Radar Operation Simulator (EROS). The effort has been devoted primarily to continuing the implementation of EROS hardware and software. The majority of the digital hardware has been designed to the circuit level of detail, and a few of the major units have been completely assembled and tested. The EROS software design is complete to the level of detail in which the major programs and file interfaces have been specified. One of these programs, a routine which sorts the data in a disk file, has been coded and debugged. Documentation has been drafted specifying how the EROS operator defines target and clutter scenarios.

Investigations have continued concerning the statistics of the clutter synthesis filters, and some of the ensuing results are reported in Section 2. The EROS implementation decision with regard to radar cross section scaling is discussed in Section 3. Section 4 describes a reallocation of the range-weighting range-integration functions from the digital hardware to the analog hardware.

2. CLUTTER DIGITAL FILTER ANALYSIS

2.1 Introduction

The use of pseudo-random numbers and 2-pole digital filters to produce synthetic radar return has been discussed in the Third, Fifth and Sixth EROS Quarterly Reports. The primary component of the random-noise input to the filters is produced by a 31-bit feedback shift register. A secondary noise source,[1] which is unavoidable but which must be taken into account, is digital truncation in the outputs of the filter's multipliers. During the past quarter, investigations of the synthetic clutter statistics have continued. A computer simulation of the shift-register random-number generator has been written, so that the theoretical predictions concerning its statistical behavior can be verified. The effects of truncation noise were studied by running simulations of the shift-register random-number generator with the digital filter. This effort is not yet complete, and the results will be described in a subsequent report.

2.2 Shift Register Simulation

The state of the shift register is defined by a 31-bit binary sequence $b_{30}\ b_{29}\ .\ .\ .\ b_0$. The behavior of the shift register is described by a transformation rule which produces the new bit pattern $b_{30}'\ b_{29}'\ .\ .\ .\ b_0'$ from the given bit pattern $b_{30}\ b_{29}\ .\ .\ .\ b_0$. Golomb's[2] theoretical development suggests three such transformation rules for the 31-bit shift register, all of which are equally recommended for producing the desired autocorrelation statistics. These transformations are described by the formula

$$b_i' = \begin{cases} b_{i-1} & i > 0 \\ b_{30} + b_u \pmod 2 & i = 0, \end{cases} \qquad (1)$$

where u = 2, 5, or 12. After each transformation the output random number ρ is produced, where

---

[1] See Section 2 of the Sixth EROS Quarterly Report for a more detailed description of both noise sources.

[2] Golomb, Solomon W., Shift Register Sequences, Holden-Day Inc., Cambridge, Mass., 1967.

TABLE I. Estimates of Autocorrelation Function of Pseudo-Random Number Generator

Lag m	$\tilde{R}_y$(u=2)	$\tilde{R}_y$(u=5)	$\tilde{R}_y$(u=12)
5	$.65 \cdot 10^{-3}$	$-1.87 \cdot 10^{-3}$	$-.79 \cdot 10^{-3}$
10	$1.02 \cdot 10^{-3}$	$.38 \cdot 10^{-3}$	$2.27 \cdot 10^{-3}$
15	$.61 \cdot 10^{-3}$	$.40 \cdot 10^{-3}$	$-.07 \cdot 10^{-3}$
20	$-.78 \cdot 10^{-3}$	$.77 \cdot 10^{-3}$	$-.75 \cdot 10^{-3}$
25	$.90 \cdot 10^{-3}$	$.53 \cdot 10^{-3}$	$-.80 \cdot 10^{-3}$
30	$.72 \cdot 10^{-3}$	$1.67 \cdot 10^{-3}$	$.83 \cdot 10^{-3}$
35	$-.22 \cdot 10^{-3}$	$1.02 \cdot 10^{-3}$	$-.26 \cdot 10^{-3}$
40	$-1.49 \cdot 10^{-3}$	$-1.17 \cdot 10^{-3}$	$-.69 \cdot 10^{-3}$
45	$-.46 \cdot 10^{-3}$	$-1.89 \cdot 10^{-3}$	$-1.52 \cdot 10^{-3}$
50	$1.53 \cdot 10^{-3}$	$.50 \cdot 10^{-3}$	$-1.16 \cdot 10^{-3}$

Notes: u = bit number of feedback bit. Sample size is 10^6.

$$\rho = (2\, b_0' - 1)\gamma \quad . \tag{2}$$

Thus the two possible random outputs are $+\gamma$ and $-\gamma$.

If $\rho(0)$, $\rho(T)$, . . . , $\rho(mT)$ . . . is the sequence of pseudo-random outputs, then the theoretical behavior of the autocorrelation function $R_\rho(mT)$ is described by

$$R_\rho(mT) = \begin{cases} \gamma^2 & m = 0 \\ \dfrac{-\gamma}{(2^{31} - 1)} & m \neq 0 \end{cases} \tag{3}$$

An experimental verification of this behavior has been performed by simulating the pseudo-random number generator (with $\gamma = 1$) on the PDP-11 computer and by calculating the autocorrelation estimate

$$\tilde{R}_\rho(mT) = \frac{1}{s} \sum_{i=1}^{s} \rho(iT)\, \rho(iT + mT) \quad , \tag{4}$$

where s is an integer denoting the sample size. Table I lists the calculation results obtained from a sample size s of 10^6 for lags m = 5, 10, 15, . . ., 50 and for the three feedback bit positions u = 2, 5, and 12.

The theoretical value $R_\rho(\text{non-0})$ is approximately 5×10^{-10} or effectively 0 for our purposes. The deviations from 0 in Table I are not surprising, because we would expect variations from the mean due to the finiteness of the sample size. However, to determine more precisely whether the deviations are unexpectedly large, a statistical test has been applied against the hypothesis that the expected value of $\rho(iT)$ $\rho(iT + mT)$ equals 0.

Since $\rho(iT)$ $\rho(iT + mT)$ assumes only the two values + 1 and - 1, the hypothesis of 0 expected value implies that

$$P[\rho(nT)\, \rho(nT + mT) = 1] = P[\rho(nT)\, \rho(nT + mT) = -1] = \frac{1}{2} \quad ,$$

where P [predicate] denotes the probability that "predicate" is true. Let the random variable x denote the number of + 1's in the sample $\{\rho(T)\, \rho(T + mT), \rho(2T)\, \rho(2T + mT), \ldots, \rho(sT)\, \rho(sT + mT)\}$. The distribution of x is the well-known binomial distribution, which implies that the mean and variance of x are sp and sp(1 - p), respectively,

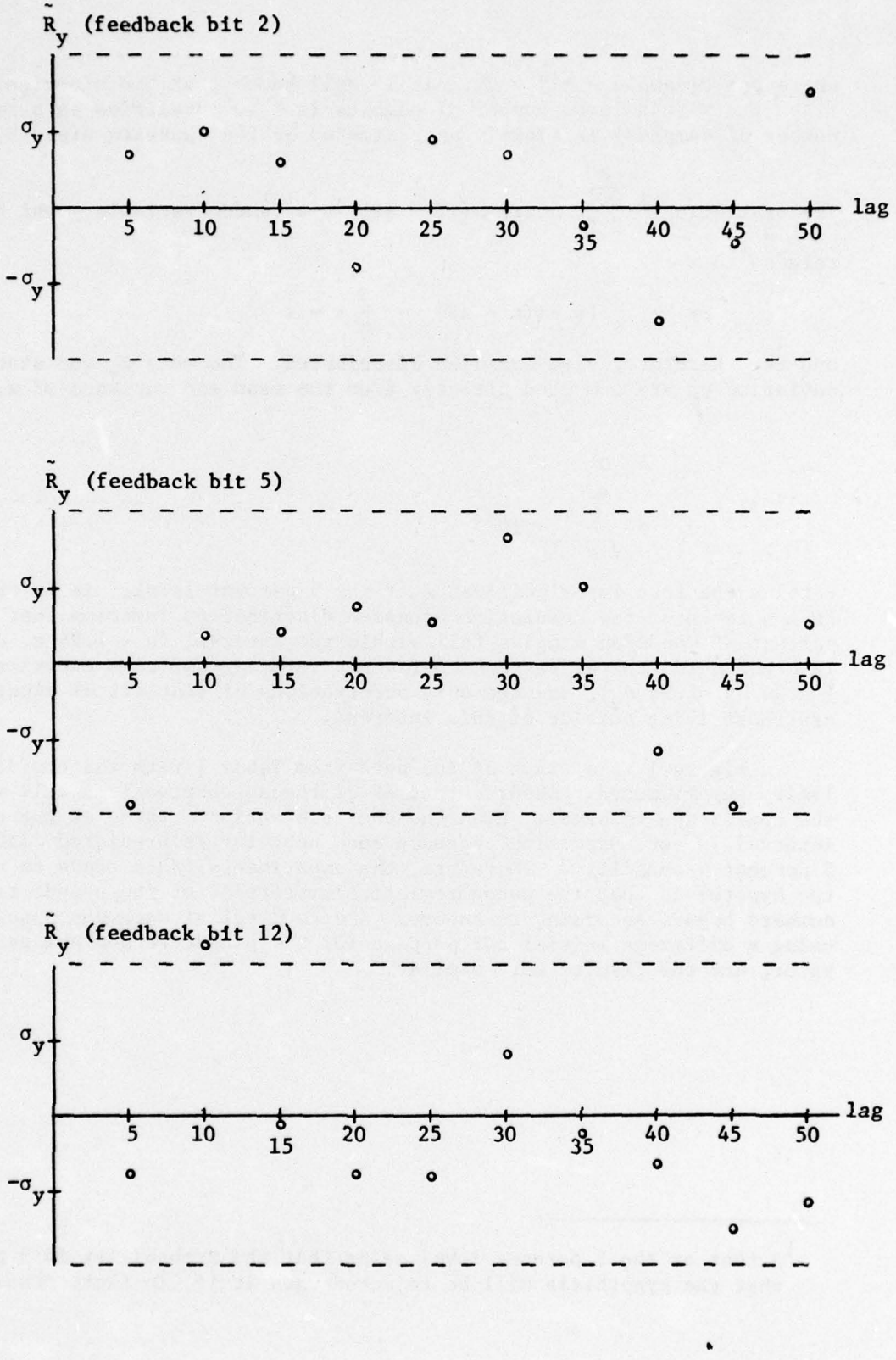

Figure 1. Estimates of Autocorrelation Function with Confidence Limits.

where $p = P[\text{sample} = +1] = \frac{1}{2}$. It is well known that the binominal distribution with a large number of samples ($s = 10^6$ qualifies as a large number of samples) is closely approximated by the Gaussian distribution.

The statistic $\frac{1}{s} \sum_{i=1}^{s} \rho(iT)\, \rho(iT + mT)$ is a random variable y which is related to x

$$y = \frac{1}{s} [x - (s - x)] = \frac{2}{s} x - 1 \quad , \tag{5}$$

and is, therefore, also Gaussian distributed. The mean μ_y and standard deviation σ_y are computed directly from the mean and variance of x.

$$\mu_y = 0$$

$$\sigma_y = \frac{1}{\sqrt{s}} = 10^{-3} \quad .$$

Setting the test for significance at the 5 percent level,[1] it is observed from a table of the cumulative Gaussian distribution function that 95 percent of Gaussian samples fall within the interval ($\mu - 1.94\ \sigma$, $\mu + 1.94\ \sigma$). In other words the 95 percent confidence interval for this experiment is ($-1.94\ \sigma_y$, $1.94\ \sigma_y$), and the only observations of statistical significance are those lying outside of this interval.

Figure 1 is a graph of the data from Table I with the confidence limits superimposed. Observe that 29 of the 30 observations fall within the confidence interval. Even the one observation outside of the confidence interval is not surprising, because such behavior is predicted with a 5 percent probability. Therefore, the experimental data tends to support the hypothesis that the autocorrelation properties of the pseudo-random numbers behave according to theory. A second set of data was obtained using a different initial bit pattern for the pseudo-random number generator, and the results were similar.

---

[1] A test at the 5 percent level means that the probability is 5 percent that the hypothesis will be rejected when it is, in fact, true.

3. RADAR CROSS SECTION SCALING

Recorded target signals maintained in EROS computer storage and synthetic clutter signals generated by the digital filters are both represented by sequences of samples. The form of each sample is a pair of binary words; the first word, I, represents the in-phase component of the sample and the second word, Q, represents the quadrature component of the sample. These signals will hereafter be called "unweighted signals" to draw the distinction between them and radar return signals. The squared amplitude, $I^2 + Q^2$, of each sample in an unweighted signal is proportional to the radar cross section and is independent of the position of the simulated contributing scatterers. Subsequent operations in EROS hardware transform unweighted signals into synthetic radar return signals by introducing azimuth dependence, performing D/A conversion, introducing range dependence, adding noise, etc.

The average squared amplitude of $\overline{A^2}$ of an unweighted signal (I_1, Q_1), (I_2, Q_2), . . . , (I_n, Q_n) is proportional to the average radar cross section σ of the scatterers being simulated. Thus

$$\sigma = K_\sigma \overline{A^2} = K_\sigma \frac{1}{n} \sum_{i=1}^{n} (I_i^2 + Q_i^2) \quad . \tag{6}$$

In order to specify K_σ for EROS implementation it is necessary to define the numerical interpretation of the bit patterns that represent I_i and Q_i. It has been found convenient to interpret each pattern as a binary fraction, where the sign bit is immediately followed by a binary point.[1] More precisely the bit pattern $b_0\ b_1\ .\ .\ .\ b_m$ (b_k equals 0 or 1) is interpreted as the number $-b_0 + (\frac{1}{2})\ b_1 + (\frac{1}{4})\ b_2 + \ .\ .\ . + (\frac{1}{2})^m\ b_m$. With this interpretation K_σ has been chosen to be 20000 such that σ in equation (6) is expressed in square meters. Therefore, the largest radar cross section that can be simulated with the current EROS implementation model approaches 20,000 square meters.

---

[1] For example, see Section 2.3 of the Fourth EROS Quarterly Report and Section 2.5 of the Fifth EROS Quarterly Report.

The application of equation (6) to recorded target signals is straight-forward. The average squared amplitude of the recording is computed as $\frac{1}{n}\sum_{i=1}^{n}(I_i^2 + Q_i^2)$. Then for a given target simulation with a specified radar cross section σ, the recording is appropriately amplified or attenuated in order to satisfy (6).

The unweighted synthetic signal from each clutter cell consists of two parts, the reflections from immobile scatterers and the reflections from moving scatterers. Equation (6) applies to both parts.

The unweighted synthetic signal from immobile scatterers is represented by a complex constant (I, Q); its average amplitude $\overline{A^2}$ is very simply $I^2 + Q^2$. To simulate a clutter cell whose immobile scatterers have a combined radar cross section σ, $\overline{A^2}$ must be chosen so that $\sigma = 20000\ \overline{A^2}$.

Two real digital filters are used in EROS implementation to simulate the return from the moving part of clutter. This pair of filters, treated as a complex digital filter, produce a sequence of signal samples (I_i, Q_i). In the Sixth EROS Quarterly Report the symbol y was used to denote the complex random process described by the sequence of filter outputs, and formulas were derived for computing the mean and variance of y.[1] The mean of y, which is not necessarily 0, is allocated to the part of the clutter return from immobile scatterers. When the mean of y is subtracted out, and the average squared amplitude of the remaining signal is computed, the result is the variance of y. Therefore, to simulate a clutter cell whose moving scatterers have a combined radar cross section σ, the variance s^2 of y must be chosen so that $\sigma = 20000\ s^2$.

---

[1] Refer to Equations (13) and (16) in Section 2.3 of the Sixth EROS Quarterly Report.

4. ANALOG HARDWARE

4.1 Analog Range Weighting

The problem caused by the conflicting requirements of high resolution and high speed in D/A conversion has been a major concern in the design of the EROS analog interface. Some of the possible solutions to this problem were treated in Section 4 of the Fourth EROS Quarterly Report. This section contained a proposed compromise solution, which left much to be desired; the conversion was to be performed with two separate D/A channels with different scale factors for the short and long radar ranges. One of the approaches which was rejected in the fourth quarterly report involved range weighting by analog multiplication after D/A conversion instead of digital multiplication before conversion. Although the baseline EROS design approach advocated exclusively digital computations for the sake of accuracy and repeatability, the advantages of analog range weighting after D/A conversion more than compensate for the loss in precision.

In the generation of the EROS baseband signal, the unweighted contributions of simulation cells defined by range rings and azimuth columns are first weighted in azimuth and summed in azimuth along each range ring. Then the azimuth sums, each representing the contribution of a single range ring, are range weighted and summed in range. The important consideration is that range weighting must be performed prior to range summing. Therefore, if range weighting is to be performed by analog multiplication after D/A conversion, then the range sum must be formed by adding analog signals after analog multiplication. This summation can be performed in an analog integrator.

In the baseline design described in Section 2 of the Frist EROS Quarterly Report, an initial range sum was formed for each transmitter modulation interval, and new sums were formed as the modulation propagated through each successive range ring. Each new sum differed from the preceeding sum by twice the range-weighted contribution of the corresponding range ring. The integrator used in the analog summation technique is reset to an arbitrary fixed level at the time of each transmitter modulation, holds at a constant value through range rings containing no targets or clutter, and changes value in each simulation range ring by an amount calibrated to be equal to twice the weighted contribution of that range ring. Thus, the output of the analog integrator is identical to the analog output of the baseline design except for the addition of an arbitrary constant. This constant is a DC level corresponding to the difference between the integrator reset level

and the initial range sum generated in the baseline design. This DC level is of no consequence, because of the bandpass signal coupling employed in the radar. Since the pass band does not extend to zero frequency, a new DC level is established at the mean value of the video waveform.

There are a number of significant benefits of analog range weighting and integration. These are enumerated below and discussed in more detail in succeeding paragraphs.

- More advantageous use of D/A converter resolution
- Simplification of digital hardware
- Simplification of software
- Simplification of analog hardware
- Reduction of bit-switching transients
- Elimination of artificial saturation
- Simplification of adapting EROS to other forms of transmitter modulation

4.2 Implementation of Analog Weighting

Twelve-bit D/A converters are available with speeds adequate to process real-time video signals. Three such converters are used: (1) to convert sign and magnitude of In-phase (I) data prior to range weighting; (2) to convert sign and magnitude and Quadrature (Q) data prior to range weighting; and (3) to convert magnitude of the range weight values. The analog output of the range weight D/A converter is multiplied by the I signal and by the Q signal in separate analog multipliers.

For video signal simulation, digital signals representing the I and Q content and range weight of successive range rings are latched into the three D/A converters at 100 nanosecond intervals. Outputs of the analog multipliers are integrated in analog integrators, which are reset periodically by pulses coincident with the transmitter modulation. Since signals from all range rings are present for equal time increments, integration with respect to time is equivalent to algebraic addition of the data from successive range rings. The integrators are also quite effective in reducing the bit-switching transients that are inherent in D/A converters. The output of the integrators are fed into variable-gain video amplifiers, which provide calibration and the addition of

adjustable simulated receiver noise. Simple band-pass filters are used to limit the video signal bandwidth to that of the radar preamplifier, and to further attenuate bit-switching transients that originate in the D/A converters.

For simulation of range-gated Doppler signals, the EROS operator selects one of the 64 range rings by means of a knob on the analog hardware. Digital signals representing the I content, Q content, and range weight of the selected range ring are latched into the D/A converters at the transmitter modulations. The range integrators have been switched out, and the range weighting analog multipliers are connected through low-pass filters to variable-gain Doppler output amplifiers.

The present method of analog range weighting lends itself readily to simulation of other types of radar modulation. In particular, the bipolar video signal of conventional pulse-Doppler radar differs from the AN/PPS-15 video in that the returns from a single range resolution cell contribute to the video signal at any given point in the interpulse interval. This signal is simulated in EROS simply by switching out the range integrator and adjusting signal and noise levels appropriately for the parameters of the radar under test. The range-gated Doppler signal for pulse modulation and for the AN/PPS-15 modulation do not differ in form, and only the adjustment of signal and noise levels is required.

4.3 Use of D/A Converter Resolution

Three high-speed 12-bit D/A converters are used to convert I data, Q data, and range weights. Reserving one bit for sign in the I and Q converters, the remaining 11 bits represent 2048 discrete amplitude levels which are proportional to the square root of instantaneous RCS. Digital scaling has been chosen such that RCS up to 20,000 m^2 can be represented in any range ring; therefore, the smallest non-zero RCS that can be represented is $20{,}000/(2048)^2 \approx .005\ m^2$.

If received power is assumed to vary as R^{-4}, then 12 bits of range weighting are sample to cover ranges from 60 m to 3000 m. If a range weighting law differing from R^{-4} is required, it may become necessary to restrict the simulation to specified range intervals or to rescale the entire problem. This limitation is reasonable, because few targets will be detectable at maximum range if received power drops much more rapidly than R^{-4}.

4.4 Hardware Simplification

The change to analog range weighting and range integration results in a substantial simplification of both digital and analog hardware. The

baseline EROS design required four high-speed digital multipliers for range weighting and four adders for integration. These have been replaced in the revised design by two analog multipliers and two integrating capacitors. The integrating capacitors also serve the important function of attenuating the converter bit-switching transients. Eight guard circuits that were required to protect against overflow in the digital multipliers and adders have been eliminated. Separation and recombination of data for two differently scaled range channels is eliminated. Alarm circuits, previously required because digital saturation in the long-range channel occurred at a much lower signal level than natural saturation of the radar receiver, are no longer required. The number of D/A converters is reduced from 6 to 3, with an accompanying reduction in the number of input latches, output filters, and calibration adjustments. Mode selection for simulation of other types of modulation and for processing video or Doppler signals is simplified.

4.5 Software Simplification

Digital software is subsequently simplified by relegation of the range weighting and range integration operations to the analog hardware. Digital scaling of range weight data and RCS data are now completely independent. This independence reduces the constraints on recorded signal levels and on digital filter parameters; the reduction of constraints in turn eliminates a complicated data edit function in the simulation preparation software. Problems of digital overflow related to range weighting have been avoided, because no digital arithmetic involving range weight is performed during simulation.

4.6 Present Status of Analog Hardware

Almost all of the components required for construction of the analog hardware have been selected and purchased. Circuits combining D/A converters, input latches, analog multipliers, and analog integrators have been breadboarded and tested. One half of the clock synchronizer has been breadboarded, and is being used in the laboratory to supply clock signals to digital circuits as they are developed. Pre-Doppler and post-audio filters have been tested. Signal insertion and extraction points in the AN/PPS-15 radar have been identified, and their impedance levels have been verified. The radar interface patchboard has been laid out for construction.

4.7 Next Quarter Plans

During the next quarter, the breadboard video and Doppler analog signal circuits will be expanded to include output amplifiers, filters,

calibration controls, mode selection switches, and impedance matching circuits. Additional synchronizer circuits will be constructed. Breadboard combinations of the A/D converters with input amplifiers and level setting adjustments will be assembled, for A/D conversion of range gate and azimuth position voltages and recorded target signals. The radar interface patchboard will be constructed to provide interconnection between EROS and the radar.

5. SUMMARY OF NEXT QUARTER PLANS

The implementation of the EROS feasibility model will continue during the next quarter. Analysis efforts will be directed toward specifications for computing the filter scaling multiplication coefficient, taking into account the contribution due to truncation noise. In addition, analyses will be performed to verify the spectral behavior of the filters. Most of the digital hardware unit assembly and unit test is scheduled for completion by the end of next quarter. Programming of the real-time software will continue with primary emphasis on the target data handling routine. The development of simulation preparation software will continue, and the plans include writing programs for clutter reference file maintenance and target signal recordings. Implementation of the analog hardware will continue, and plans call for completion of the radar-interface unit.

HEADQUARTERS
US ARMY ELECTRONICS COMMAND
FORT MONMOUTH, NJ 07703

AMSEL-CT-R

TITLE OF REPORT: Environment and Radar Operation Simulator (EROS)
CONTRACT NUMBER: DAAB-74-C-0272
CONTRACTOR: Georgia Institute of Technology

DISTRIBUTION LIST

	NR. OF COPIES
Defense Documentation Center ATTN: DDC-TCA Cameron Station (Bldg 5) Alexandria, VA 22314	1
Defense Intelligence Agency ATTN: DIADT-3C Washington, DC 20301	1
Dir, National Security Agency ATTN: TDL Ft George G. Meade, MD 20755	1
Dir, Defense Nuclear Agency ATTN: Technical Library Washington, DC 20305	1
Naval Ship Engineering Center ATTN: Code 6179B Prince Georges Center Bldg Hyattsville, MD 20782	1
Cdr, Naval Electronics Lab Center ATTN: Library San Diego, CA 92152	1
Cdr, US Naval Ordnance Lab ATTN: Technical Library White Oak, Silver Spring, MD 20910	1
Commandant, Marine Corps HQ US Marine Corps ATTN: Code A04C Washington, DC 20380	1

AMSEL-CT-R
Distribution List for Contract DAAB07-74-C-0272, Georgia Inst of Technology

	NR. OF COPIES
Communications-Electronics Division Development Center Marine Corps Dev & Educ Command Quantico, VA 22134	1
Cdr, US Naval Weapons Lab ATTN: KEB-2F(FENN) Dahlgren, VA 22448	1
Rome Air Development Center ATTN: Documents Library (TDLD) Griffiss AFB, NY 13440	1
HQ ESD (TRI) L. G. Hanscom Field Bedford, MA 01730	1
Air Force Avionics Laboratory ATTN: AFAL/DOT (STINFO) Wright-Patterson AFB, OH 45433	1
Armament Development & Test Center ATTN: SSLT Eglin AFB, FL 32542	1
HQ, Air Force Systems Command ATTN: DLTE Andrews AFB Washington, DC 20331	1
Air Force Weapons Laboratory ATTN: Technical Library (SUL) Kirtland AFB, NM 87117	1
Cdr, US Army Training & Doctrine Cmd ATTN: ATTS-X Fort Monroe, VA 23651	1
HQDA (DAFD-CN) Washington, DC 20310	1
HQDA (DACE-ED) Washington, DC 20314	1

AMSEL-CT-R
Distribution List for Contract DAAB07-74-C-0272, Georgia Inst of Technology

	NR. OF COPIES
Ofc, Asst Secy of the Army (R&D) ATTN: Assistant for Research Rm 3-E-379, The Pentagon Washington, DC 20310	1
Cdr, US Army Training & Doctrine Cmd ATTN: ATCD-SI Fort Monroe, VA 23651	1
HQDA (DARD-ARP/Dr. R. B. Watson) Washington, DC 20310	1
Cdr, US Army Materiel Command ATTN: AMCRD-O 5001 Eisenhower Ave Alexandria, VA 22333	1
Cdr, US Army R&D Group (Far East) APO, San Francisco, CA 96343	1
Cdr, USA Missile Command Redstone Scientific Info Center ATTN: Ch, Document Section Redstone Arsenal, AL 35809	1
Cdr, US Army Training & Doctrine Cmd ATTN: ATCE Fort Monroe, VA 23651	1
Cdr, USA Weapons Command ATTN: AMSWE-REF Rock Island, IL 61201	1
Cdr, US Army Combined Arms Combat Dev Activity ATTN: ATCAIC Fort Leavenworth, KS 66027	1
HQ, USA Aviation Systems Command ATTN: AMSAV-C-AD P. O. Box 209 St. Louis, MO 63166	1

AMSEL-CT-R
Distribution List for Contract DAAB07-74-C-0272, Georgia Inst of Technology

	NR. OF COPIES
Cdr, Harry Diamond Laboratories ATTN: Library Washington, DC 20438	1
Cdr, USA Foreign Sci & Tech Cen ATTN: AMXST-IS1 220 Seventh St., NE Charlottesville, VA 22901	1
Cdr, USA Picatinny Arsenal ATTN: SMUPA-VC5 (Mr. P. Kisatsky) Bldg 350 Dover, NJ 07801	1
Cdr, Frankford Arsenal ATTN: Library, H1300, Bldg 51-2 Philadelphia, PA 19137	1
Crd, White Sands Missile Range ATTN: STEWS-RE-10 (Mr. G. Galos) White Sands Missile Range, NM 88002	1
Dir, USA Ballistic Research Lab ATTN: AMXBR-VL (Mr. D. L. Riggotti) Aberdeen Proving Ground, MD 21005	1
Cdr, USA Mat & Mech Rsch Center ATTN: AMXMR-ATL (Tech Library Br) Watertown, MA 02172	1
President, USA Artillery Board Fort Sill, OK 73503	1
Cdr, Aberdeen Proving Ground ATTN: Technical Library, Bldg 313 Aberdeen Proving Ground, MD 21005	1
Cdr, USA Electronic Proving Ground ATTN: STEEP-MT Fort Huachuca, AZ 85613	1
Cdr, USASA Test & Evaluation Center Fort Huachuca, AZ 85613	1

AMSEL-CT-R
Distribution List for Contract DAAB07-74-C-0272, Georgia Inst of Technology

	NR. OF COPIES
USA Research Office - Durham ATTN: Dr. Robert J. Lontz Box CM, Duke Station Durham, NC 27706	1
Cdr, USA Mobility Eqpt R&D Center ATTN: Tech Docu Cntr, Bldg 315 Fort Belvoir, VA 22060	
USA Security Agency ATTN: IARD Arlington Hall Sta, Bldg 420 Arlington, VA 22212	1
Cdr, USA Tank-Automotive Command ATTN: AMSTA-RH-FL Warren, MI 48090	1
Technical Support Directorate ATTN: Technical Library, Bldg 3330 Edgewood Arsenal, MD 21010	1
Cdr, US Army Combined Arms Combat Dev Activity ATTN: ATCACC Fort Leavenworth, KS 66027	1
Cdr, USA Dugway Proving Ground Library ATTN: STEDP-TL (Tech Library) Dugway, UT 84022	1
Cdr, Yuma Proving Ground ATTN: STEYP-AD (Tech Library) Yuma, AZ 85364	1
Cdr, US Army Materiel Command ATTN: AMCRD-R 5001 Eisenhower Avenue Alexandria, VA 22333	1
Commandant, US Army Infantry Sch ATTN: ATSIN-CTD Fort Benning, GA 31905	1

AMSEL-CT-R
Distribution List for Contract DAAB07-74-C-0272, Georgia Inst of Technology

	NR. OF COPIES
Commandant, USA Field Artillery School ATTN: Target Acquisition Dept Fort Sill, OK 73503	1
Cdr, USA Systems Analysis Agency ATTN: AMSRD-AMB (Mr. A. Reid) Aberdeen Proving Ground, MD 21005	1
Cdr, USA Tank-Automotive Cmd ATTN: AMSTA-Z (Dr. J. Parks) Warren, MI 48090	1
Ch, Missile EW Technical Area EW Laboratory (ECOM) White Sands Missile Range, NM 88002	1
Ch, Intelligence Mat Dev Ofc EW Laboratory (ECOM) Fort Holabird, MD 21219	1
NASA Sci & Tech Info Facility ATTN: Acquisitions Br (S-AK/DL) P. O. Box 33 College Park, MD 20740	1
Target Signature Analysis Center Willow Run Labs - Inst of Science & Technology University of Michigan P. O. Box 618 Ann Arbor, MI 48107	1
Remote Area Conflict Info Center Battelle Memorial Institute 505 King Avenue Columbus, OH 43201	1
Martin Marietta Corporation ATTN: MS 0452 (Lynes) P. O. Box 179 Denver, CO 80201	1
Cdr, Rome Air Development Center ATTN: Mr. John C. Cleary/OCSA Griffiss AFB, NY 13441	1

AMSEL-CT-R

Distribution List for Contract DAAB07-74-C-0272, Georgia Inst of Technology

NR. OF COPIES

Cdr, US Army Electronics Command
Fort Monmouth, NJ 07703

1	AMSEL-NV-D	1	AMSEL-VL-D	1	AMSEL-MA-MP	1	AMSEL-PA
1	AMSEL-WL-D	1	AMSEL-CT-R	1	AMSEL-MS-TI	1	AMSEL-RD
1	AMSEL-NL-D	1	AMSEL-SI-CB	1	AMSEL-GG-RD	1	TDC-LNO

This contract is supervised by Radar Technical Area, Combat Surveillance and Target Acquisition Laboratory, US Army Electronics Command, Fort Monmouth, New Jersey 07703. Tel: Eatontown, NJ, Area Code (201) 596-1407.